An Analytical Relationship Between Compressor Thermofluid Efficiency and Manifold Acoustic Modes

R. Singh

J. J. Nieter

AN ANALYTICAL RELATIONSHIP
BETWEEN COMPRESSOR THERMOFLUID EFFICIENCY
AND MANIFOLD ACOUSTIC MODES

by

Rajendra Singh
Associate Professor and Director
Fluid Power Laboratory

Jeffrey J. Nieter*
Graduate Research Associate

Department of Mechanical Engineering
The Ohio State University
206 W. 18th Avenue, Columbus, Ohio 43210

*Currently Assistant Research Engineer at the United Technologies Research Center
East Hartford, Connecticut 06108

ABSTRACT

Basic thermofluid processes of a positive displacement compressor are strongly dependent upon the acoustic behavior of the manifolds. Hence manifold tuning is very important so as to increase flow capacity while reducing energy consumption and fluidborne noise; recently we developed a computer simulation program used to examine the tuning phenomena analytically. However, such numerical predictions may not lead directly to either a physical understanding of the tuning phenomena or to simple analytical expressions which could be used by a designer for finding the most suitable solution. This paper presents a hypothesis that relates in general functional form the flow and energy efficiencies and pressure pulsations of a compressor to the acoustic modes of the manifolds. Application is demonstrated through the example case of a two-cylinder compressor suction manifold. The results of the linear system study undertaken here match well with the predictions of the computer simulation program and experiment. The hypothesis set forth in this paper should lead future investigators to develop the important relationships between compressor performance and manifold design.

1. INTRODUCTION

The idea of tuning work producing or consuming positive displacement machines such as internal combustion engines and gas compressors is not new. Since designers often use experimental or empirical approaches, the concept employed for one machine may not be valid for other fluid machines. However, there seems to be a general concensus that by chosing a proper inlet and/or exhaust manifold geometry one can tune or detune the cylinder which could lead to a significant improvement in mass flow rates and thermodynamic efficiency [1-6]. A closed form mathematical solution is not feasible because of nonlinearities and strong dynamic interactions between various processes and components. Consequently, a computer simulation program is required which would numerically solve the governing equations simultaneously, in an iterative mode in order to account for the back pressure effect [7-10]. However, such numerical predictions often do not lead directly to either a physical understanding of the tuning phenomena or to simple analytical expressions which could be used by a designer for finding the optimal solution.

The purpose of this paper is to present a modal analysis theorem which relates essential thermofluid efficiency indices to the acoustic pressure modes of the inlet or exhaust system. Application will be demonstrated through the example case of a two-cylinder compressor suction manifold.

2. SCOPE

Recently we developed a computer simulation procedure which includes the manifold back pressure effect to investigate and explain the tuning phenomena for a single or two-cylinder reciprocating compressor [10]. A symmetric suction manifold system for a two-cylinder refrigeration compressor was considered as the example case in this tuning study. Results for flow efficiency η_F, energy efficiency η_E, and peak-to- peak pressure pulsations at the valve exit Δp_V were presented in terms of the acoustic natural frequencies ω_r of the manifold system. Predicted results compared reasonably well with experimental data.

Now we are interested in developing an analytical relationship. Accordingly, we assume the manifold system to be a linear acoustic system, excited at the valves by the mass flow through the valves. Assume that the back pressure effect is negligible in the sense that the input forcing function is not corrected by the resulting manifold pressure p_V. However, we assume that thermofluid efficiency indices η_F and η_E are dependent variables and somehow related to Δp_V. Now our aim is to develop a relationship between manifold acoustic properties and thermofluid efficiencies. First a hypothesis will be given, and then relationships will be explored for the same example case used for the computer simulation study [10]. For the linear system analysis, a lumped parameter approach (in contrast to the distributed parameter approach used in the simulation study [10]) will be adopted for clarity and ease. Results of the analytical procedure presented here will be compared with the results of the previous study [10].

3. FORMULATION

Consider a positive displacement machine such as a compressor with baseline (or operating point) values η_{E0}, η_{F0}, and Δp_{V0}. Now let us assume that we are interested in achieving maximum possible efficiency and minimum possible fluidborne noise through suitable modifications to the manifold geometry. Let us characterize the manifold acoustic properties by acoustic natural frequency ω_r and displacement mode shape $\{U_r\}$ where r is the modal index. Consider changes $\Delta\eta_E$, $\Delta\eta_F$, and Δp_V as dependent response variables such that linear system assumptions are still valid. It has been shown [11] as given below that acoustic pressure at position j in the manifold can be given by the acoustic modal expansion (see Nomenclature for identification of symbols)

$$\tilde{p}_j(t) = \sum_r u_r^j h_r(t) \tag{1}$$

$$\Delta p_V = K_p \sum_{n=1}^{\infty} |\tilde{H}_{1,n}| \tag{2}$$

where $\tilde{H}_{1,n}$ is a transfer function, as defined in Equation (21) of Section 5, and given in the modal expansion form. Based on intuition and the results of our previous simulation study, we hypothesize that

$$\Delta\eta_F = K_F \sum_{n=1}^{\infty} \mathrm{Re}(\tilde{H}_{1,n}) \tag{3}$$

$$\Delta\eta_E = K_E \sum_{n=1}^{\infty} \mathrm{Im}(\tilde{H}_{1,n}) \tag{4}$$

Since changes in thermofluid efficiencies of compressors can be strongly dependent upon pressure pulsations in the manifolds, the forms of (3) and (4) seem reasonable. We further hypothesize that a general thermofluid efficiency $\tilde{\eta}$ in complex form can be described as follows: (Here we assume that η_F and η_E are coincidence and quadratic forms of $\tilde{\eta}$.)

$$\tilde{\eta} = \eta_F + i\eta_E \tag{5}$$

$$\tilde{\eta} = \tilde{\eta}_0 + \Delta\tilde{\eta} = (\eta_{F0} + \Delta\eta_F) + i(\eta_{E0} + \Delta\eta_E) \tag{6}$$

and this can be nondimensionalized by $\eta_0 = |\tilde{\eta}_0|$ as

$$\tilde{\eta}^* = \frac{\tilde{\eta}}{\eta_0} = \tilde{\eta}_0^* + \frac{\Delta\tilde{\eta}}{\eta_0} \tag{7}$$

Using equations (3-7) we get

$$\tilde{\eta}^* = \eta_F^* + i\eta_E^* \tag{8a}$$

$$\eta_F^* = \eta_{F0}^* + \frac{K_F}{\eta_0} \sum_{n=1}^{\infty} \mathrm{Re}(\tilde{H}_{1,n}) \tag{8b}$$

$$\eta_E^* = \eta_{E0}^* + \frac{K_E}{\eta_0} \sum_{n=1}^{\infty} \mathrm{Im}(\tilde{H}_{1,n}) \tag{8c}$$

If $K_F = K_E = K_\eta$, then

$$\tilde{\eta}^* = \tilde{\eta}_0^* + \frac{K_\eta}{\eta_0} \sum_{n=1}^{\infty} \tilde{H}_{1,n} \tag{9}$$

Also, taking this approach with Δp_V gives

$$\Delta p_V^* = \frac{\Delta p_V}{p_0} = \frac{K_p}{p_0} \sum_{n=1}^{\infty} |\tilde{H}_{1,n}| \tag{10}$$

4. MULTICYLINDER CASE

Compressor manifolds have been modeled as lumped acoustic systems [11,13] where acoustic volume displacement is the response, excited by the input volume velocity. The governing equation for an N dimensional system is as follows

$$[m_a]\{\ddot{\tilde{x}}_j(t)\}+[d_a]\{\dot{\tilde{x}}_j(t)\}+[k_a]\{\tilde{x}_j(t)\} = \{\tilde{f}_j(t)\} \tag{11}$$

In general, $\{\tilde{x}(t)\}$ and $\{\tilde{f}(t)\}$ are periodic,

$$\{\tilde{x}_j(t)\} = \sum_{n=1}^{\infty} \{\tilde{X}_{j,n}\} e^{in\omega t} \tag{12}$$

$$\{\tilde{f}_j(t)\} = \sum_{n=1}^{\infty} \{\tilde{F}_{j,n}\} e^{in\omega t} \tag{13}$$

and here we limit $[d_a]$ to the proportional case. Solving the homogenous form of (11) yields N pairs of distinct roots [10,14]

$$\tilde{s}_r = -\zeta_r\omega_r \pm i\omega_r\sqrt{1-\zeta_r^2}\,, \quad r = 1,2,\ldots,N, \tag{14}$$

where ω_r is the natural frequency. The acoustic volume displacement mode shapes are then computed from

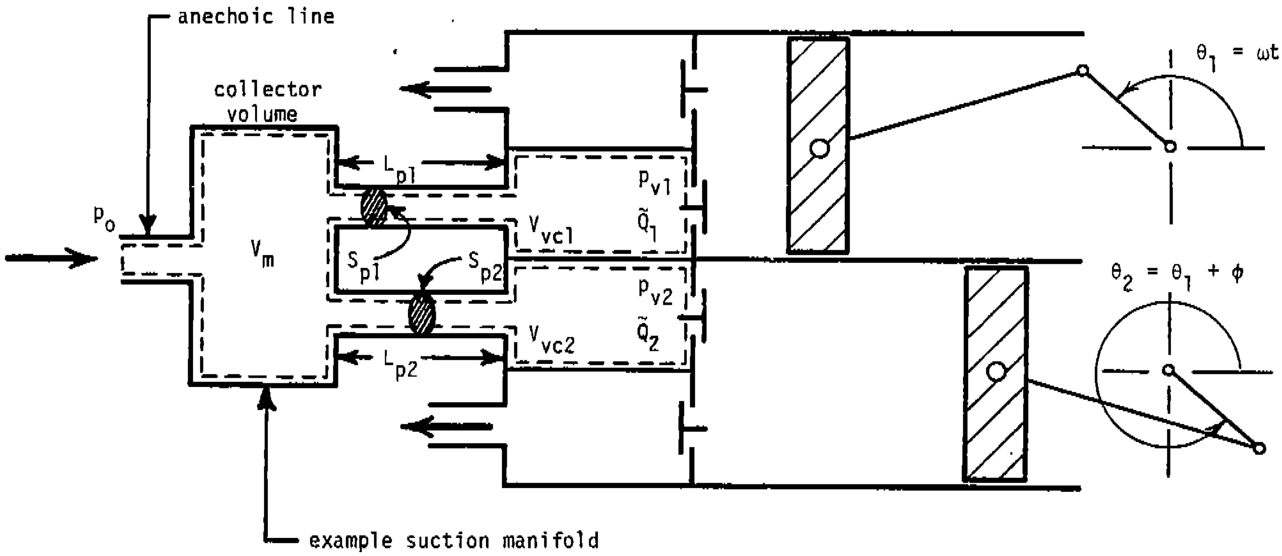

Figure 1. Example Case: Two-Cylinder Compressor and Symmetric Suction Manifold

$$\left[\tilde{s}_r^2[m_a] + \tilde{s}_r[d_a] + [k_a]\right]\{U_r\} = \{0\} \tag{15}$$

Using the modal summation theorem,

$$\{\tilde{X}_j\} = \sum_{r=1}^{N} \gamma_r \{u_r^j\} \ , \tag{16}$$

and the orthogonality conditions of the $\{U_r\}$, the frequency response solution to (11) is [10]

$$\{\tilde{X}_{j,n}\} = \begin{Bmatrix}\tilde{X}_{2,n}\\ \tilde{X}_{4,n}\end{Bmatrix} = \sum_{r=1}^{N} \frac{\{U_r\}^T\{\tilde{F}_{j,n}\}\{U_r\}}{[1-(\frac{n\omega}{\omega_r})^2+i2\zeta_r(\frac{n\omega}{\omega_r})]k_r} \tag{17}$$

Equation (17) indicates that the acoustic volume displacement is given by the acoustic modal properties of the manifold system [10,11,13].

5. TWO-CYLINDER EXAMPLE CASE

Now consider a two-cylinder symmetric compressor manifold; Figure 1 is a schematic of this example case. The acoustic natural frequencies for our example case are given in the dimensionless form as [10,11,13]

$$\xi_r = \frac{\omega_r}{\omega_c} \tag{18}$$

in Table 1.

Table 1. Natural Frequencies of the Example Case

ξ_r	Discrete Model	Continuous Model
ξ_1	1.738	1.633
ξ_2	3.469	3.271

The acoustic volume displacement mode shapes are computed from lumped parameter theory as [10,11,13]

$$[U] = [\{U_1\}\{U_2\}] = \begin{bmatrix} u_1^1 & u_2^1\\ u_1^2 & u_2^2\end{bmatrix} = \begin{bmatrix}1 & 1\\ 1 & -1\end{bmatrix} . \tag{19}$$

The corresponding acoustic pressure mode shapes are given in Figure 2; excellent agreement with the results from the continuous system model [10,13] are evident. The forcing function for this example case can be described in terms of the acoustic volume velocities at the valves [10,11,13]

$$\{\tilde{F}_{j,n}\} = \begin{Bmatrix}\tilde{F}_{2,n}\\ \tilde{F}_{4,n}\end{Bmatrix} = \frac{\rho c^2}{in\omega}\begin{Bmatrix}\tilde{Q}_{1,n}/V_1\\ \frac{\tilde{Q}_{2,n}}{V_5}\, e^{i(n\phi+\pi)}\end{Bmatrix} \tag{20}$$

Thus, for the symmetric manifold in Figure 1, with $\phi = \pi$ and $\tilde{Q}_{1,n} = \tilde{Q}_{2,n}e^{i(n+1)\pi}$, Equation (17) can be described in nondimensional transfer function form [13]:

$$\begin{Bmatrix}\tilde{H}_{1,n}\\ \tilde{H}_{2,n}\end{Bmatrix} = \frac{\rho c^2}{V_1}\sum_{r=1}^{2}\frac{\{U_r\}^T\begin{Bmatrix}1\\ \cos[(n+1)\pi]\end{Bmatrix}\{U_r\}}{[1-(\frac{n\omega}{\omega_r})^2+i2\zeta_r(\frac{n\omega}{\omega_r})]k_r} \tag{21}$$

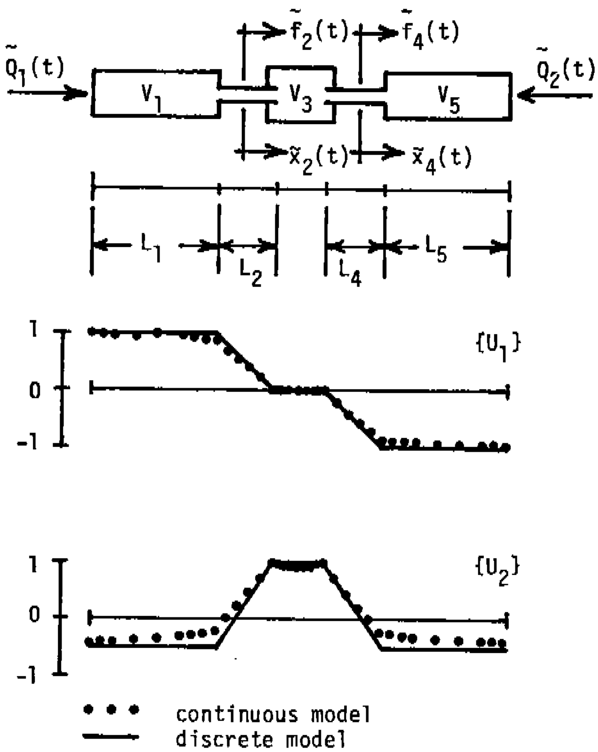

Figure 2 Acoustic Pressure Mode Shapes of the Example Suction Manifold

6. RESULTS & DISCUSSION

The hypothesis set forth in Section 3 has been compared graphically to the tuning results obtained in a recent study using the computer simulation program [10,13]. The flow efficiencies plotted in Figures 3-6 are the real part of Equation (8), the energy efficiencies plotted in Figures 7-10 are the imaginary part of Equation (8), and the pressure pulsations plotted in Figures 11-14 are from Equation (10). All harmonics should be included in $\tilde{H}_{1,n}(\omega)$, however since the first two harmonics are dominant in $\{\bar{Q}_j(t)\}$, and in order to simplify analysis, we have considered only the cases n=1 and n=2. For n=1 (refer to Figures 3, 5, 7, 9, 11, and 13), only the first acoustic mode is excited for this example case. This is because the modal participation of the second mode when n=1 is zero. Also, the modal participation of the first mode when n=2 is zero. In general, odd harmonics in a symmetric two-cylinder manifold excite the first acoustic mode while even harmonics excite the second mode [10,11,13]. For n=2 (refer to Figures 4, 6, 8, 10, 12, and 14), only the second acoustic mode is excited as described above. Realistic damping [10-13] is included in the manifold model for Figures 5, 6, 9, 10, 13, and 14. In all figures, both the undamped cases and the damped cases, the modal expansion descriptions in Equations (8) and (10) 'fit' the simulation data very well. Experimental data included in Figures 5, 9, and 13 for n=1 also substantiates the comparison. However, the experimental data was collected over a long period of time so that it was difficult to maintain the same compressor design and operating conditions, and therefore, there is some scatter to the experimental data. No experimental data is, however, available when the second mode is excited. In all graphs, our modal expansion descriptions do not predict the dependent variable fluctuations occurring in the simulation data at higher frequency ratios than $\xi_1 = 1$ and $\xi_2 = 2$ because we have considered excitations at only n=1 and n=2. Higher harmonics (apparently n=3 and n=6) also excite acoustic modes in the example manifold. We have used only n=1 and n=2 to show the strong relationship between manifold acoustic modes and thermofluid efficiencies and pressure pulsations at the lower, dominant harmonics. In general, all harmonics are present and therefore, we write our modal expansion descriptions in Equations (8) and (10) as summations of all possible harmonics.

CONCLUSIONS

The results presented here show that a strong relationship exists between compressor thermofluid efficiencies, pressure pulsations, and the acoustic modes of the compressor manifolds. We have hypothesized a general functional relationship to describe such results based on an acoustic modal expansion function of the manifold. Though this functional relationship is not a totally complete one, it points the way for future research which could ultimately make manifold tuning a relatively quick procedure and design optimization possible.

ACKNOWLEDGEMENTS

We would like to acknowledge the much appreciated financial support of Copeland Corporation, Sidney, Ohio, and the assistance of Fran Simpson and Young-In Moon.

REFERENCES

[1] F. K. Bannister, 1958, Proc. Inst. Mech. Engrs., 117 (13), 375-397. Induction Ramming of Small High Speed Air Compressor.

[2] R. A. Stien and J. A. Eibling, 1962, Proceedings of X International Congress of Refrigeration, Washington, D.C., 191-207. Improving Compressor Performance by Discharge Tuning.

[3] H. A. Jaspers, 1969, Proceedings of XII International Congress of Refrigeration, Madrid, Spain, Paper No. 3.54, 839-846. Special Suction Lines Influencing The Volumetric Efficiency of Reciprocating Compressors.

[4] H. W. Engelman, 1953, Ph.D. Thesis, University of Wisconsin. Surge Phenomena in Engine Scavenging.

[5] W. W. Eberhard, 1971, M.Sc. Thesis, The Ohio State University. A Mathematical Model of Ramcharging Intake Manifolds for Four-Stroke Diesel Engines.

[6] A. L. Schwallie, 1972, M.Sc. Thesis, The Ohio State University. Verification of a Mathematical Model for Intake Manifold Design.

[7] J. Brablik, 1974, Proceedings of The Second Purdue Compressor Technology Conference, 151-158. Computer Simulation of the Working Process in the Cylinder of a Reciprocating Compressor with Piping System.

[8] F. Laville and W. Soedel, 1978, J. Acoust. Soc. Am., 63 (S-1). Thoughts on the Effect of Acoustic Back Pressures on Engine Performance.

[9] D. C. Karnop, H. A. Dwyer, and D. L. Margolis, 1975, SAE Paper No. 750708. Computer Prediction of Power and Noise for Two-Stroke Engines with Power Tuned, Silenced Exhausts.

[10] J. J. Nieter and R. Singh, 1984, J. Sound Vib., 97(3), in press. A Computer Simulation Study of Compressor Tuning Phenomena.

[11] R. Singh and W. Soedel, 1979, J. Sound Vib., 64(3), 387-402. Interpretation of Gas Oscillations in Multicylinder Fluid Machinery Manifolds by Using Lumped Parameter Descriptions.

[12] R. Singh and W. Soedel, 1978, J. Sound Vib., 57(3), 449-452. Assessment of Fluid-Induced Damping in Refrigeration Machinery Manifolds.

[13] J. J. Nieter, 1983, M.Sc. Thesis, The Ohio State University. A Computer Simulation and Modal Analysis Study of Compressor Manifolds and Tuning Phenomena.

[14] J. J. Nieter and R. Singh, 1982, J. Acoust. Soc. Am., 72(2), 319-326. Acoustic Modal Analysis Experiment.

NOMENCLATURE

c	speed of sound
d_a	acoustic element damping, $d_a = m_a \zeta_a \sqrt{2\pi\mu\omega/\rho S}$
d_r	acoustic modal damping, $d_r = [U_r]^T[d_a][U_r]$
i	imaginary number, $i = \sqrt{-1}$
h_r	modal expansion function
f	forcing function of acoustic system
k_a	acoustic element stiffness, $k_a = \rho c^2/V$
k_r	acoustic modal stiffness, $k_r = [U_r]^T[k_a][U_r]$
m_a	acoustic element mass, $m_a = \rho L/S$
m_r	acoustic modal mass, $m_r = [U_r]^T[m_a][U_r]$
n	harmonic number
p	pressure
s	complex root of homogeneous equation
t	time
u	element of eigenvector or mode shape
x	acoustic volume displacement
F	amplitude coefficient in forcing function
H	nondimensional modal expansion transfer function
K	constant coefficient in modal expansion relationships
L	length of acoustic mass element pipe
N	number of cylinders and acoustic modes
Q	acoustic volume velocity
S	cross-sectional area of acoustic mass element pipe
U	eigenvector or mode shape
V	volume of acoustic stiffness element
X	amplitude coefficient in volume displacement function
γ_r	modal summation coefficient
ζ_a	empirical acoustic damping coefficient
ζ_r	acoustic modal damping ratio, $\zeta_r = d_r/(2m_r\omega_r)$
η	efficiency
μ	viscosity
ξ_r	frequency ratio, $\xi_r = \omega_r/\omega_c$
ρ	density
ϕ	kinematic phase angle of cylinders
ω	frequency (rad/sec)
ω_c	crank frequency
ω_r	acoustic natural frequency, $\omega_r^2 = k_r/m_r$

Subscripts

1	cylinder or acoustic element
2	cylinder or acoustic element
a	acoustic element
c	crank frequency
j	cylinder index
n	harmonic index
o	reference state
p	pressure
r	modal index
E	energy
F	flow
N	Nth position for last cylinder
V	valve

Superscripts

j	element position of eigenvector or mode shape
T	transpose of matrix or vector
*	nondimensional variable
~	complex quantity

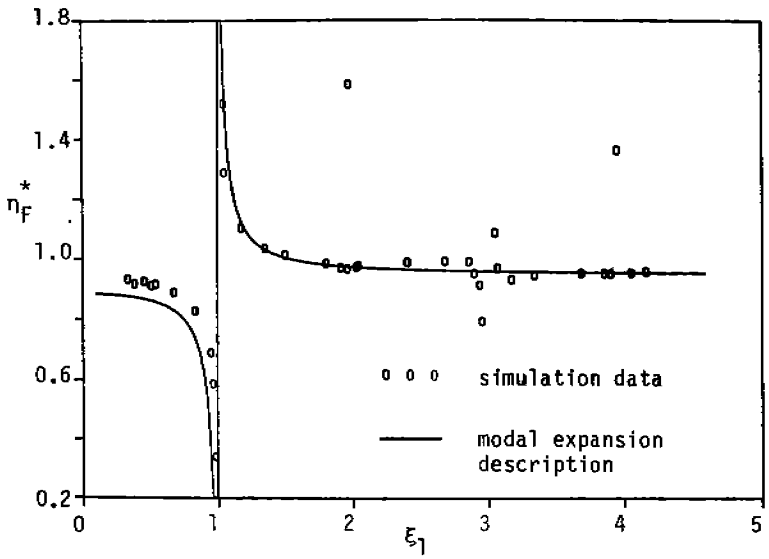

Figure 3 η_F^* Variation with ξ_1 (undamped)

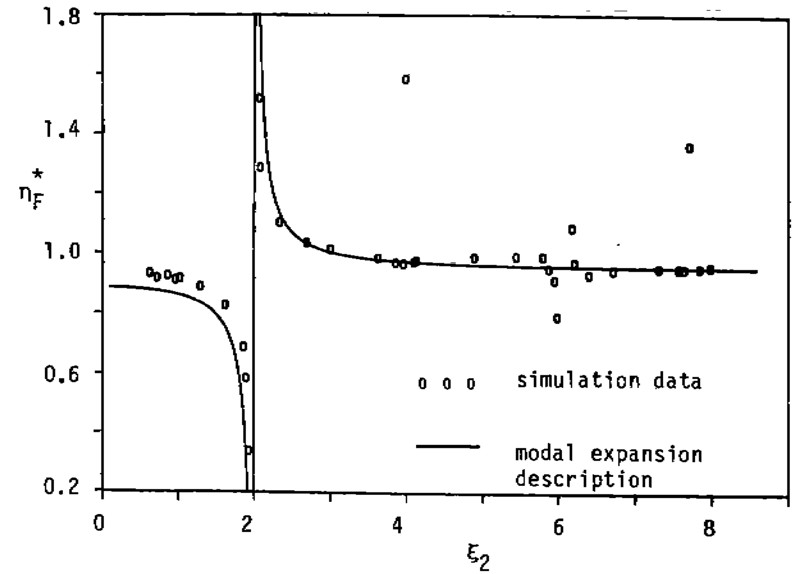

Figure 4 η_F^* Variation with ξ_2 (undamped)

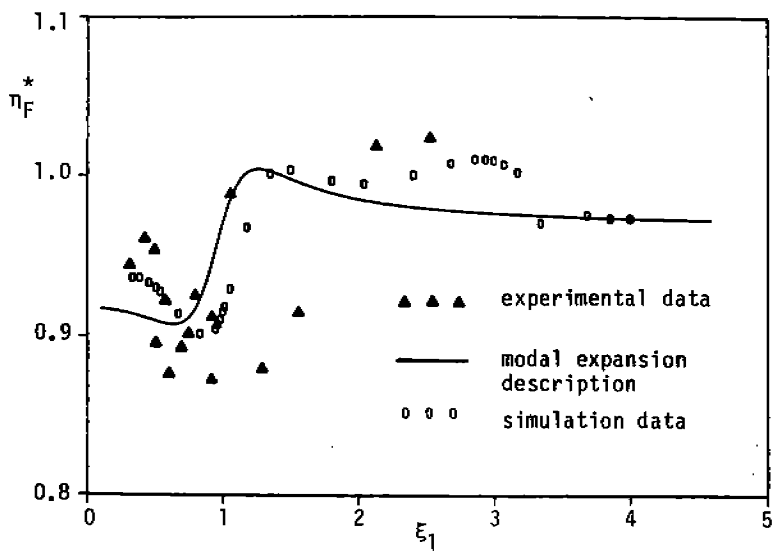

Figure 5 η_F^* Variation with ξ_1 (damped)

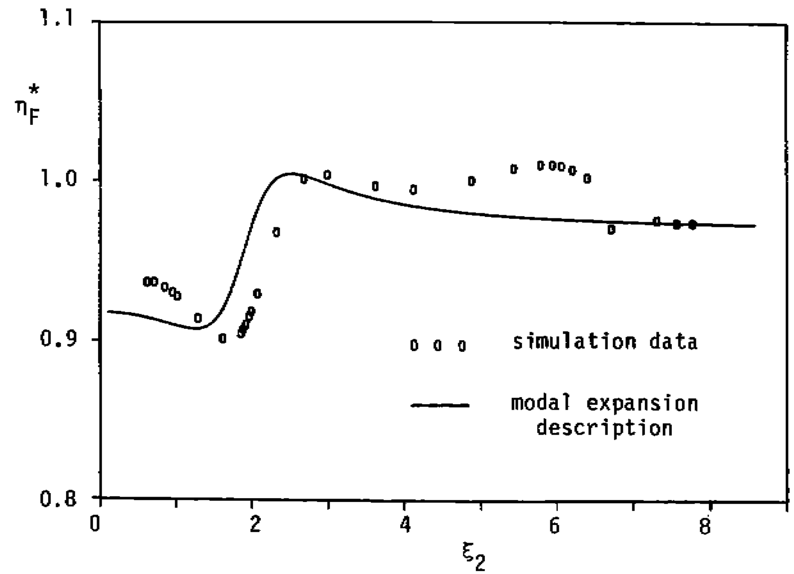

Figure 6 η_F^* Variation with ξ_2 (damped)

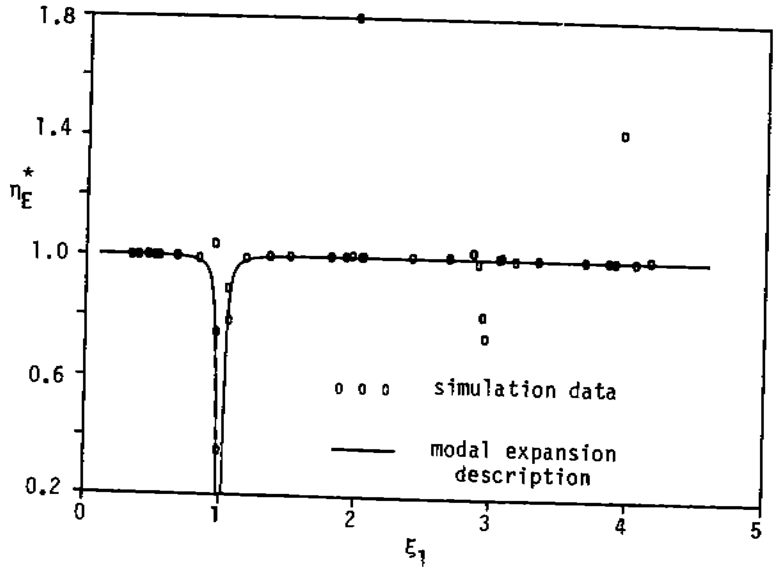

Figure 7 η_E^* Variation with ξ_1 (undamped)

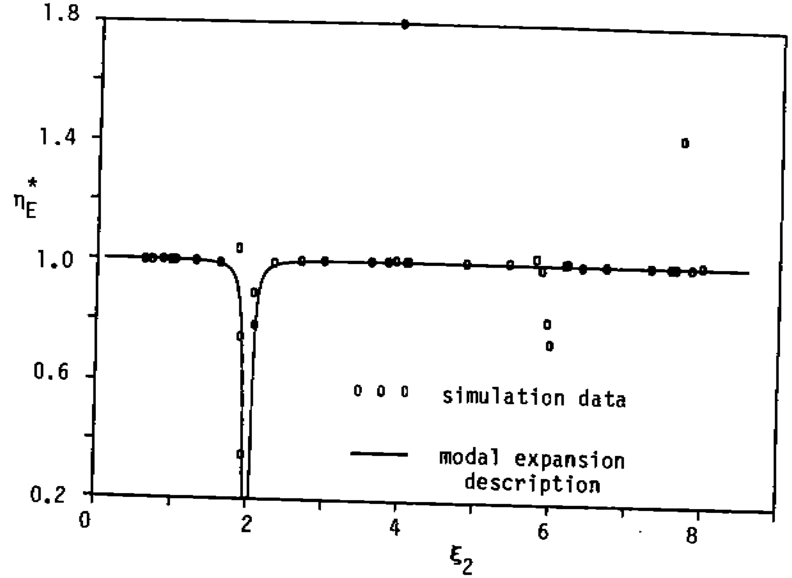

Figure 8 η_E^* Variation with ξ_2 (undamped)

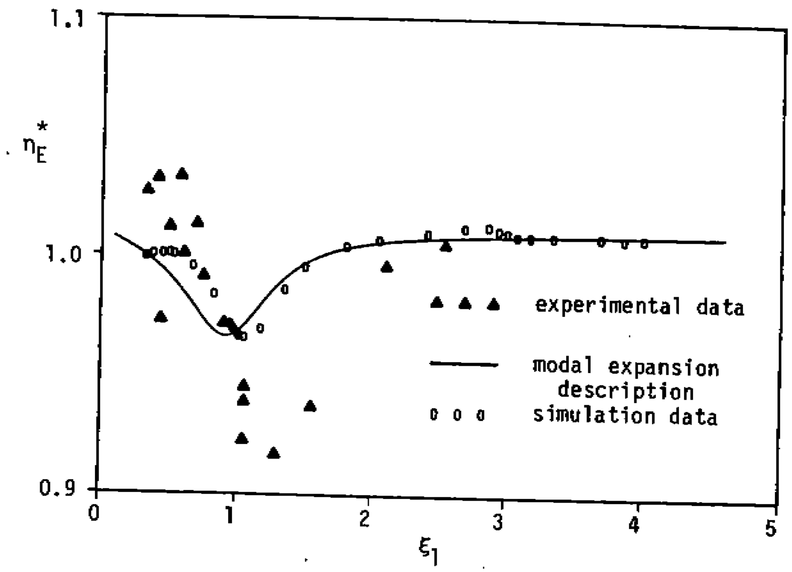

Figure 9 η_E^* Variation with ξ_1 (damped)

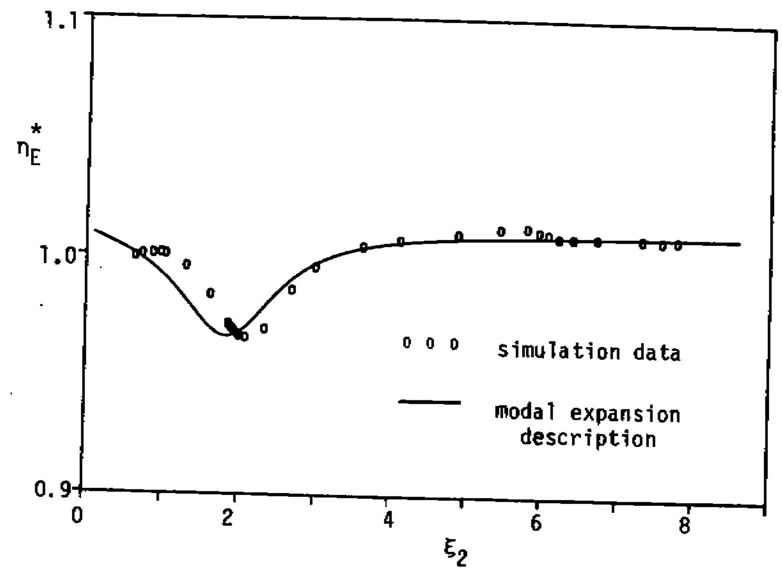

Figure 10 η_E^* Variation with ξ_2 (damped)

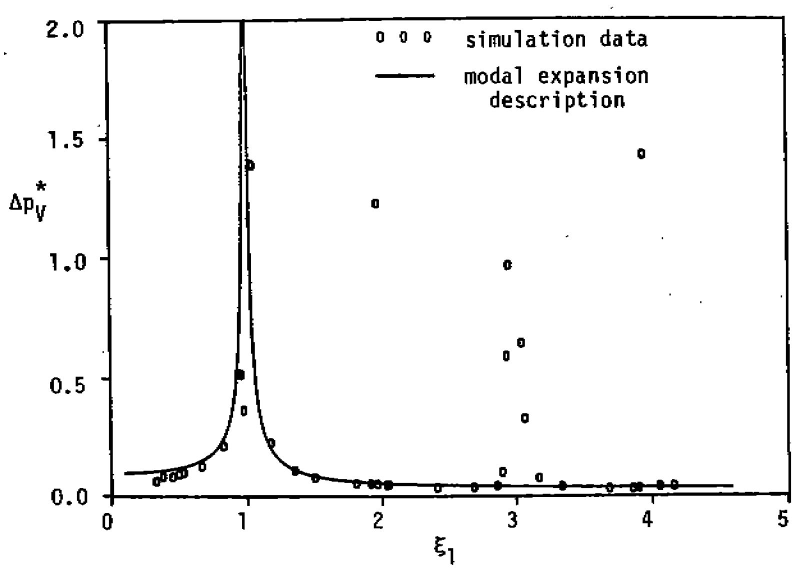

Figure 11 Δp_V^* Variation with ξ_1 (undamped)

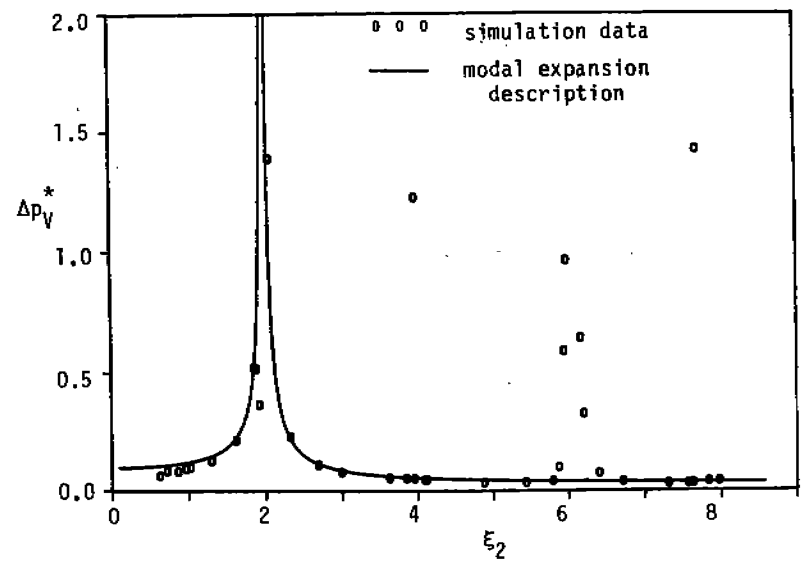

Figure 12 Δp_V^* Variation with ξ_2 (undamped)

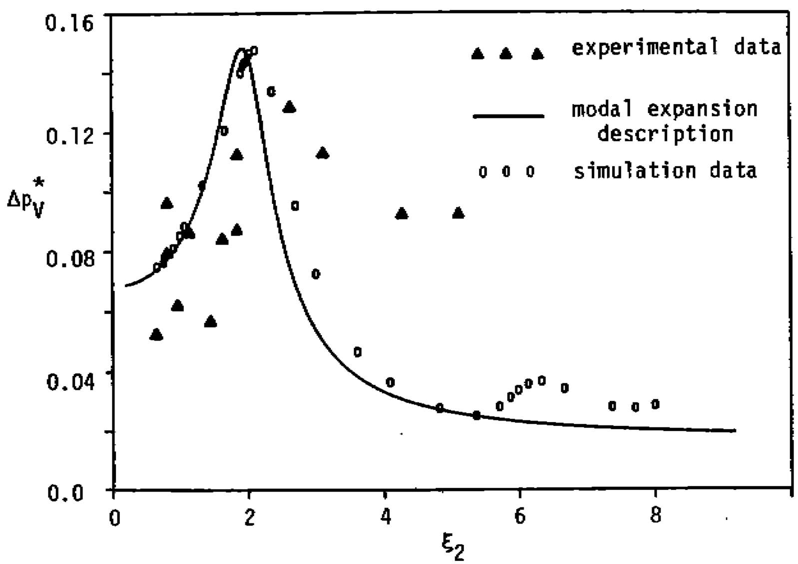

Figure 13 Δp_V^* Variation with ξ_2 (damped)

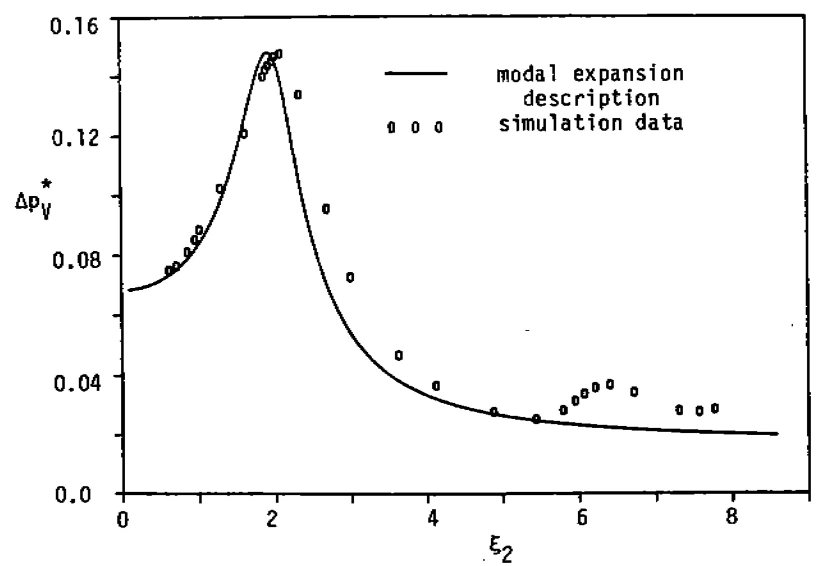

Figure 14 Δp_V^* Variation with ξ_2 (damped)